

# Magnetoelastic effects in frustrated magnets

## Investigation of $\text{LiGa}_x\text{In}_{1-x}\text{Cr}_4\text{O}_8$ "breathing" pyrochlores

Rafal Wawrzynczak

Supervisors:

Martin Böhm

Tom Fennell

Michel Kenzelmann

Gøran Nilsen

November 10, 2015

# Table of contents

"Breathing" pyrochlores

Techniques

Powder diffraction

$\text{LiInCr}_4\text{O}_8$

$\text{LiGaCr}_4\text{O}_8$

$\text{LiGa}_{0.95}\text{In}_{0.05}\text{Cr}_4\text{O}_8$

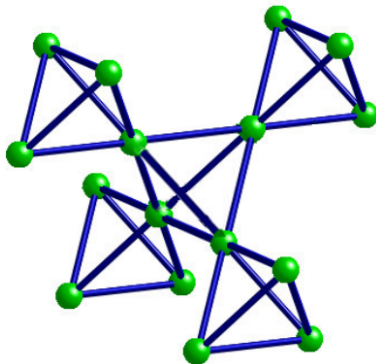
Future perspectives

# Pyrochlore lattice

**Pyrochlore lattice** composed of corner-sharing tetrahedra formed by cations.

Most important examples of compounds realizing pyrochlore lattice are:

- ▶ pyrochlores  $A_2B_2X_7$ , where  $A$  and  $B$  sites form the tetrahedra
- ▶ spinels  $AB_2X_4$ , where  $B$  site displays a pyrochlore lattice



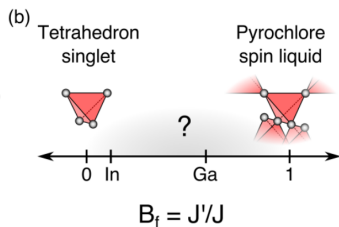
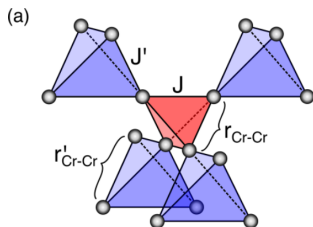
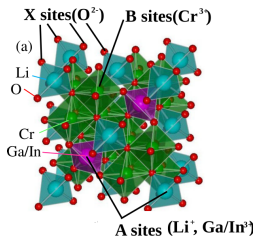
# "Breathing" pyrochlore

$\text{LiGa}_x\text{In}_{1-x}\text{Cr}_4\text{O}_8$  (spinel)  
**antiferromagnetic** exchange  
interaction between  $\text{Cr}^{3+}$   
spins ( $S = \frac{3}{2}$ ) placed on the  
corners of tetrahedra. A site  
populated by  $\text{Li}^+$ ,  $\text{Ga}^{3+}$  or  $\text{In}^{3+}$   
cations.

Okamoto et al., 2013

Nilsen et al., 2015

Cations are placed alternatively  
to minimize electrostatic energy.



# "Breathing" pyrochlore

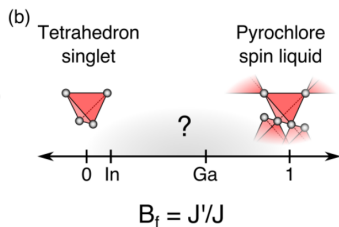
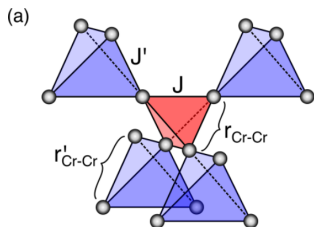
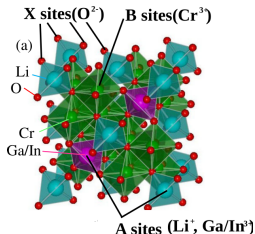
Exchange interactions between  $\text{Cr}^{3+}$  cations are very sensitive to the distance between the ions.

Composition	$r'/r$	$B_f = J'/J$
$\text{LiGaCr}_4\text{O}_8$	1.03	0.6
$\text{LiInCr}_4\text{O}_8$	1.05	0.1

Okamoto et al., 2013

Nilsen et al., 2015

Cations are placed alternatively to minimize electrostatic energy.



# Our main objectives are to determine:

- ▶ crystalline structure
- ▶ magnetic structure
- ▶ structural and magnetic phase transitions
- ▶ role of spin-lattice coupling

in  $\text{LiGa}_x\text{In}_{1-x}\text{Cr}_4\text{O}_8$  "breathing" pyrochlores.

# Powder diffraction(CW)

## HRPT(PSI)

Bragg's condition:

$$\lambda = 2d_{hkl} \sin \theta$$

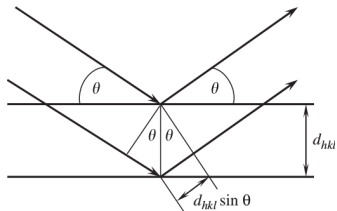


Figure : Source: [1].

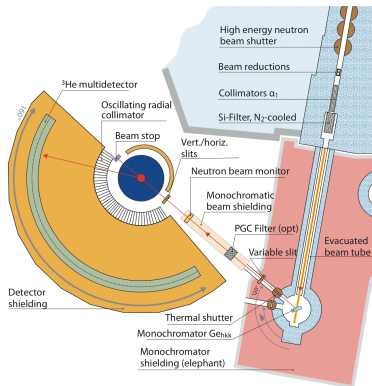


Figure : Layout of HRPT diffractometer at PSI. Source: [2].

# Powder diffraction(CW)

D20(ILL)

Bragg's condition:

$$\lambda = 2d_{hkl} \sin \theta$$

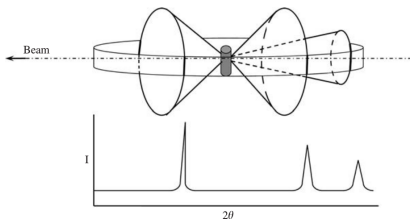


Figure : Source: [1].

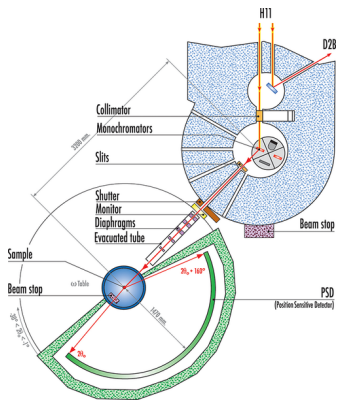


Figure : Layout of D20 diffractometer at ILL. Source: [3].



# Powder diffraction(TOF)

WISH(ISIS)

Bragg's condition:

$$d_{hkl} = \frac{ht}{2mL \sin \theta}$$

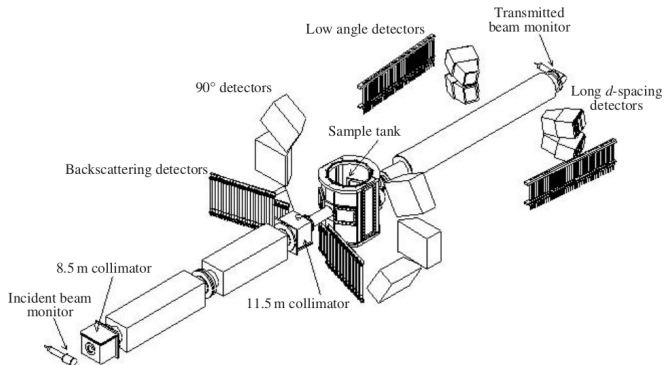


Figure : Layout of typical TOF diffractometer. Source: [1]

# Powder diffractometry

## Constant wavelength vs time-of-flight

### Constant wavelength

- ▶ **peaks are simpler to model**
- ▶ incident beam is better characterized
- ▶ simpler data storage and reduction
- ▶ straightforward absorption and extinction correction
- ▶ fine tuning of the resolution during the experiment

### Time-of-flight

- ▶ whole incoming beam spectrum is utilized
- ▶ data are collected to large  $Q$ -values (small  $d$ -spacings)
- ▶ **very high resolution can be achieved by long flight paths**
- ▶ **resolution is constant across whole pattern**
- ▶ possibility of reducing parasitic scattering from sample environment

# Powder diffractometry

## Constant wavelength vs time-of-flight - asymmetry

### Constant wavelength

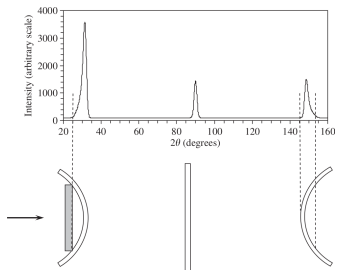


Figure : Asymmetry of Bragg peaks in CW powder diffraction.  
Source: [1].

$$FWHM^2 = U \tan^2 \theta + V \tan \theta + W \quad \frac{\Delta d}{d} = \left[ \Delta \theta^2 \cot^2 \theta + \frac{\Delta t^2}{t^2} + \frac{\Delta L^2}{L^2} \right]$$

### Time-of-flight

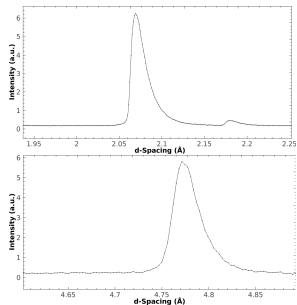


Figure : Shape of the peaks in TOF powder diffraction pattern.

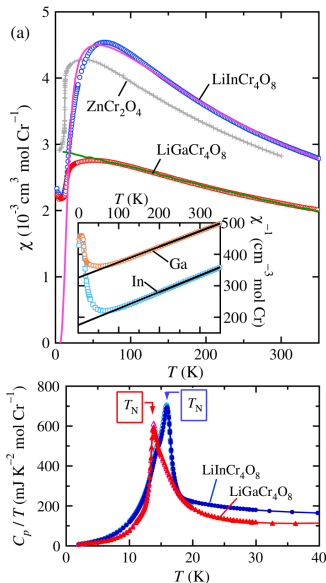
# Previous results

## Magnetic susceptibility and heat capacity

### $\text{LiInCr}_4\text{O}_8$ :

- ▶ rapid decrease of  $\chi$  above 65 K - opening of a spin gap
- ▶ energy gap estimated as close to 4.9 meV
- ▶ structural phase transition at  $\sim 16$  K
- ▶ magnetic phase transition at  $\sim 14$  K

Okamoto et al., 2013



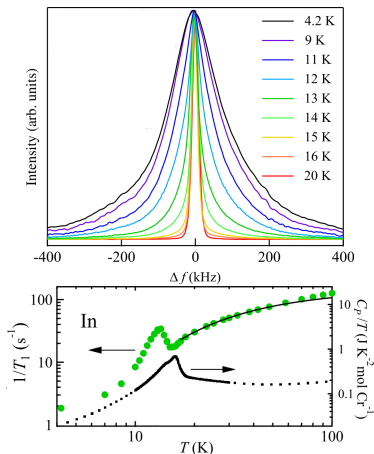
# Previous results

## NMR

### $\text{LiInCr}_4\text{O}_8$ :

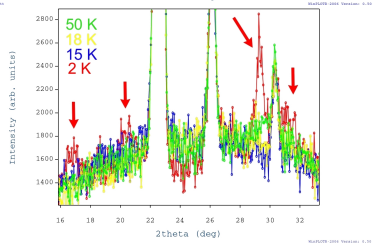
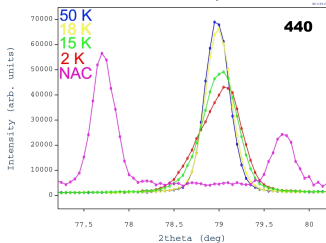
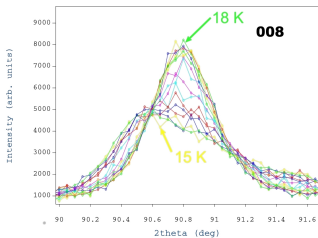
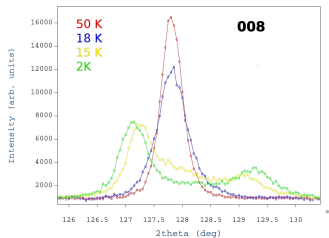
- ▶  $1/T_1$  suggest a singlet ground state with a gap of 2.7 meV
- ▶ second order AFM transition at 13 K preceded by structural transition releasing frustration

Tanaka et al., 2014



# HRPT - PSI(20-24/07/15)

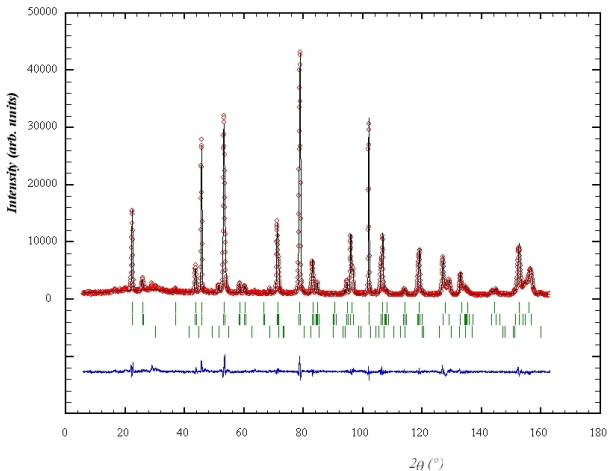
$\text{LiInCr}_4\text{O}_8$



# HRPT - PSI(20-24/07/15)

LiInCr4O8

HRPT, LiInCr4O8, corefinement 1.886A\_1.494A 2K normalized CELL: 8.40470 8.40470 8.40470 90.0000 90.0000 90.00



# HRPT - PSI(20-24/07/15)

$\text{LiInCr}_4\text{O}_8$

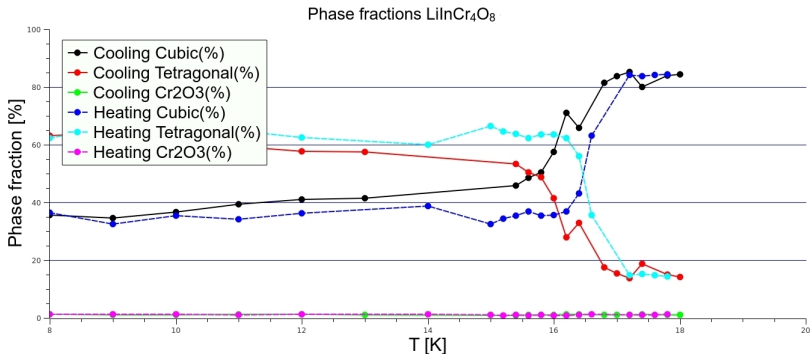


Figure : Temperature dependence of a phase fractions retrieved from Rietveld refinement.



# D20 - ILL(28-29/07/15)

$\text{LiInCr}_4\text{O}_8$

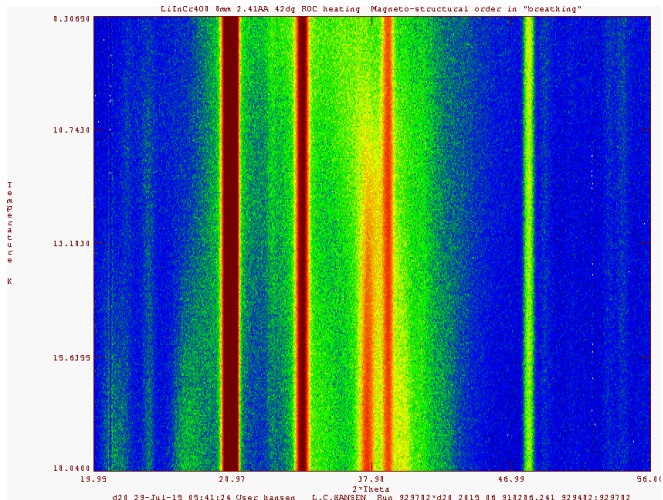


Figure : Temperature dependence of low-angle features from pattern gathered with  $\lambda = 2.41 \text{ \AA}$ .

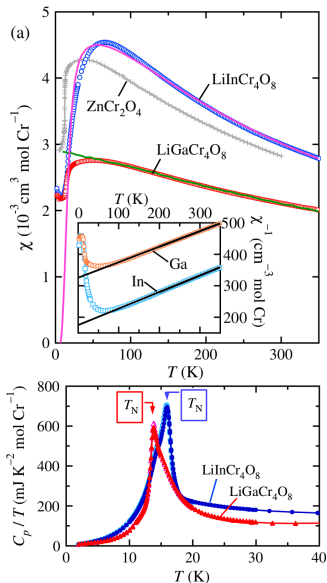
# Previous results

## Magnetic susceptibility and heat capacity

### LiGaCr<sub>4</sub>O<sub>8</sub>:

- ▶ broad peak at  $\approx 45$  K  
-development of AFM short range order
- ▶ steep decrease at  $\approx 14$  K  
-long range order sets in
- ▶ sharp peak in heat capacity at 13.8 K indicating structural phase transition

Okamoto et al., 2013

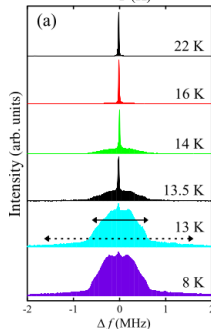
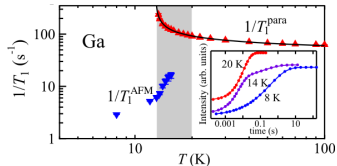
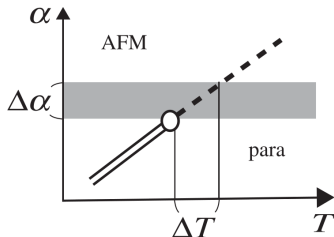


# Previous results

## NMR

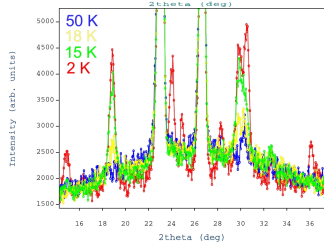
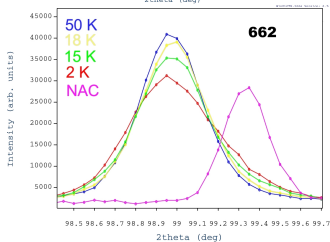
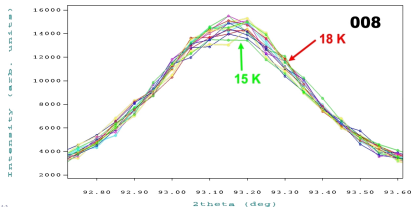
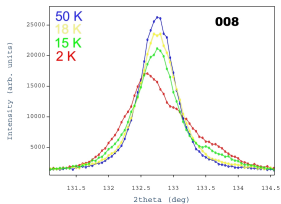
### LiGaCr<sub>4</sub>O<sub>8</sub>:

- ▶ first order AFM transition
- ▶ in the vicinity of tricritical point



# HRPT - PSI(20-24/07/15)

LiGaCr<sub>4</sub>O<sub>8</sub>



# HRPT - PSI(20-24/07/15)

LiGaCr<sub>4</sub>O<sub>8</sub>

HRPT, LinCr4O8, corefinement 1.886A\_1.494A 2K normalized CELL: 8.40470 8.40470 8.40470 90.0000 90.0000 90.00

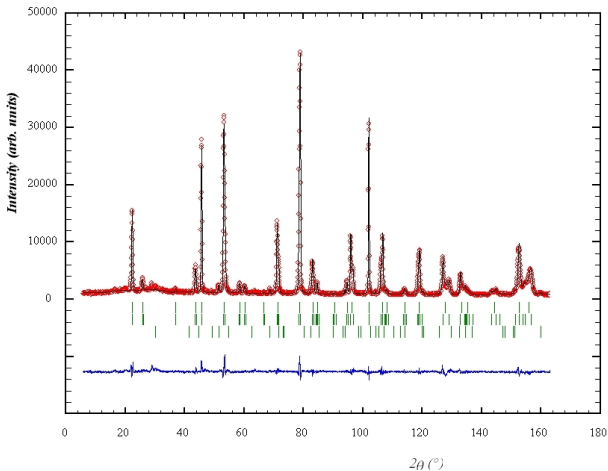
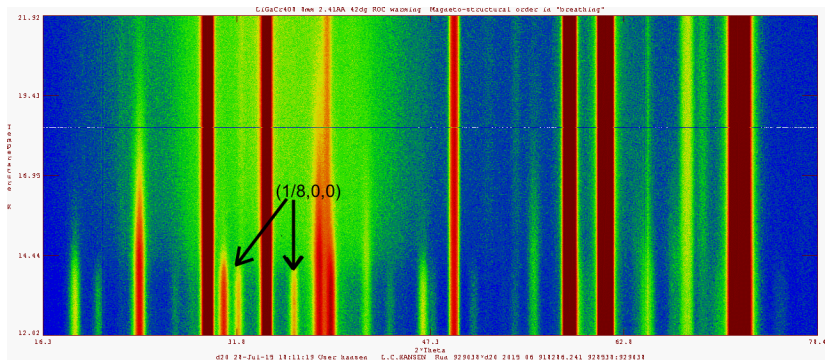


Figure : Rietveld refinement profile of 1.886 Å at 2 K with  $\chi^2 = 5.13$ .

# D20 - ILL(28-29/07/15)

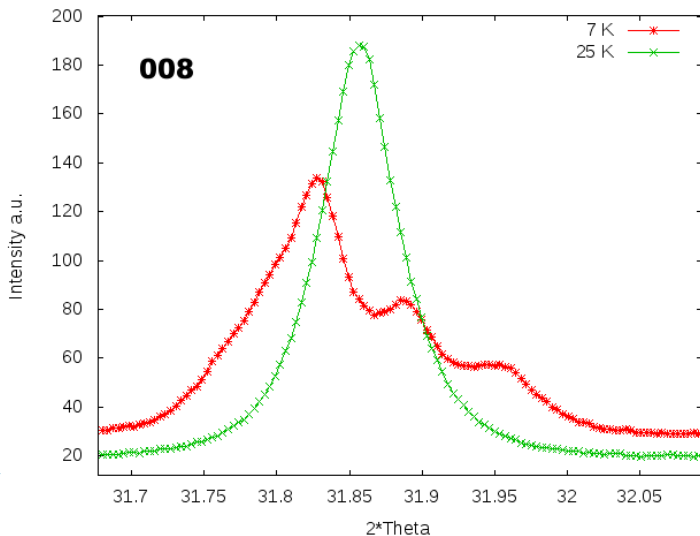
LiGaCr<sub>4</sub>O<sub>8</sub>



**Figure :** Temperature dependence of low-angle features from pattern gathered with  $\lambda = 2.41 \text{ \AA}$ . Two peaks were indexed as corresponding to  $(1/8,0,0)$   $k$ -vector.

# MS BEAMLINE - PSI(27-29/10/15)

LiGaCr<sub>4</sub>O<sub>8</sub>



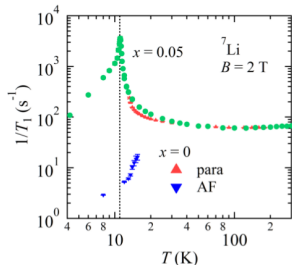
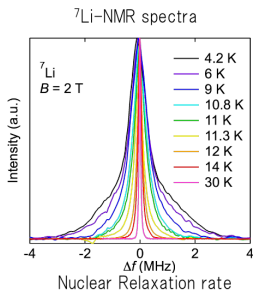
# Previous results

## NMR

**LiGa<sub>0.95</sub>In<sub>0.05</sub>Cr<sub>4</sub>O<sub>8</sub>:**

- ▶ second order AFM transition

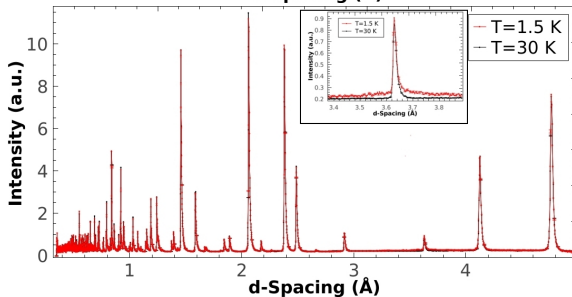
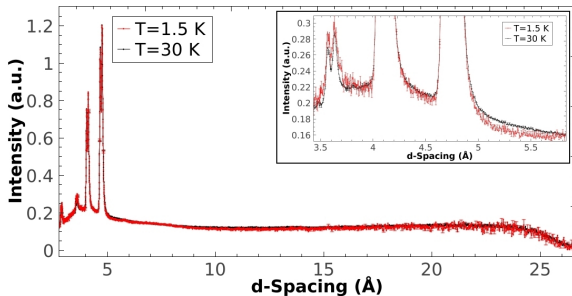
Tanaka et al., not published.





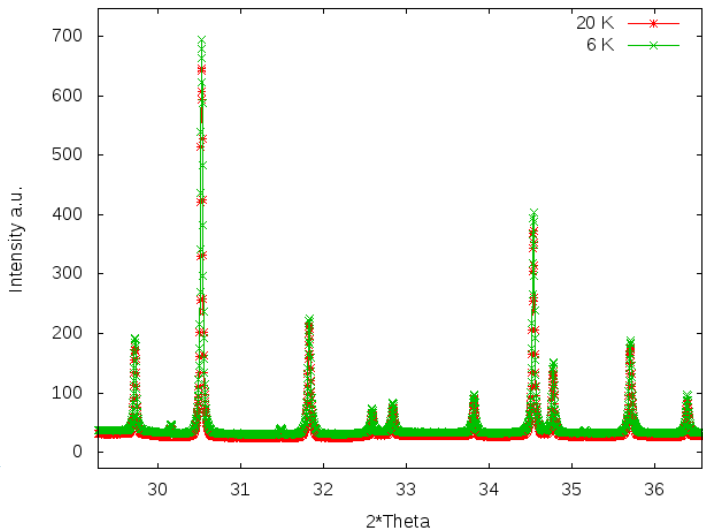
# WISH - ISIS(11-12/10/15)

$\text{LiGa}_{0.95}\text{In}_{0.05}\text{Cr}_4\text{O}_8$



# MS BEAMLINE - PSI(27-29/10/15)

$\text{LiGa}_{0.95}\text{In}_{0.05}\text{Cr}_4\text{O}_8$



# Future perspectives

- ▶ determine ordered low  $T$  magnetic structure in  $\text{LiGaCr}_4\text{O}_8$
- ▶ AC magnetic susceptibility measurements on  $\text{LiGa}_{0.95}\text{In}_{0.05}\text{Cr}_4\text{O}_8$  sample to confirm presence of spin glass phase
- ▶ perform single crystal experiments as soon as such a samples will be available

# References

[1] E.H. Kisi, C.J. Howard, *Applications of neutron powder diffraction*, Oxford University Press, Oxford, 2008.

[2] <http://www.psi.ch/>

[3] <http://www.ill.eu/>

# Magnetoelastic effects in frustrated magnets

## Investigation of $\text{LiGa}_x\text{In}_{1-x}\text{Cr}_4\text{O}_8$ "breathing" pyrochlores

Rafal Wawrzynczak

Supervisors:

Martin Böhm

Tom Fennell

Michel Kenzelmann

Gøran Nilsen

November 10, 2015